

CONFIDENTIAL

Copy 26  
RM A55C24

UNCLASSIFIED

NACA

# RESEARCH MEMORANDUM

LIFT, DRAG, AND STATIC LONGITUDINAL STABILITY  
CHARACTERISTICS OF FOUR AIRPLANE-LIKE  
CONFIGURATIONS AT MACH NUMBERS

FROM 3.00 TO 6.28

By Stanford E. Neice, Thomas J. Wong,  
and Charles A. Hermach

Ames Aeronautical Laboratory  
Moffett Field, Calif. **COPY**

APR 28 1955

LANGLEY AERONAUTICAL LABORATORY  
LIBRARY, NACA  
LANGLEY FIELD, VIRGINIA

CLASSIFIED DOCUMENT

This material contains information affecting the National Defense of the United States within the meaning of the espionage laws, Title 18, U.S.C., Secs. 793 and 794, the transmission or revelation of which in any manner to an unauthorized person is prohibited by law.

NATIONAL ADVISORY COMMITTEE  
FOR AERONAUTICS

WASHINGTON

April 25, 1955

UNCLASSIFIED

CONFIDENTIAL

NACA RM A55C24

CLASSIFICATION CHANGED

UNCLASSIFIED

To

Authority of TPA #49 Date 5-21-81 cam



UNCLASSIFIED

NATIONAL ADVISORY COMMITTEE FOR AERONAUTICS

RESEARCH MEMORANDUM

## LIFT, DRAG, AND STATIC LONGITUDINAL STABILITY

## CHARACTERISTICS OF FOUR AIRPLANE-LIKE

## CONFIGURATIONS AT MACH NUMBERS

FROM 3.00 TO 6.28

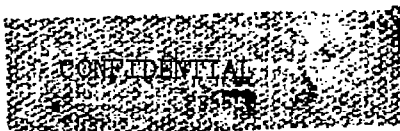
By Stanford E. Neice, Thomas J. Wong,  
and Charles A. Hermach

## SUMMARY

Lift, drag, and pitching-moment coefficients, lift-drag ratios, and center-of-pressure positions for four airplane-like configurations were determined from tests at Mach numbers from 3.00 to 6.28 and angles of attack up to  $15^\circ$ . One basic configuration consisted of trapezoidal-wing and -tail surfaces mounted on a cylindrical afterbody with a fineness-ratio-3 tangent-ogive nose. The second basic configuration, designed to have lower drag and higher lift-drag ratios, consisted of triangular-wing and -tail surfaces, which have the same spans and plan-form areas as the trapezoidal-wing model, but with more highly swept leading edges, mounted on a cylindrical afterbody with a fineness-ratio-5 "minimum-drag" nose. The third configuration was the trapezoidal-wing model modified to have a fineness-ratio-5 minimum-drag nose. The fourth configuration was the triangular-wing model with the minimum-drag nose modified to include a nose radius one-tenth of the afterbody radius. Wing and tail sections of all four configurations had rounded leading edges to reduce the effect of local aerodynamic heating.

Throughout the range of test Mach numbers, the maximum lift-drag ratios of the basic triangular-wing configuration were about 18 to 24 percent higher than those of the basic trapezoidal-wing model. About 7- to 11-percent increase in maximum lift-drag ratio was obtained by replacing the fineness-ratio-3 ogival nose of the basic trapezoidal-wing model with the fineness-ratio-5 minimum-drag nose. Increasing the nose bluntness of the triangular-wing model resulted in a decrease of about 5 percent or less in the maximum lift-drag ratio. The greatest decrease occurred at the highest test Mach number.

UNCLASSIFIED



## INTRODUCTION

An airplane-like configuration, which consisted of trapezoidal-wing and -tail surfaces mounted on a cylindrical afterbody with a fineness-ratio-3 ogival nose (refs. 1 and 2), has been investigated as a suitable vehicle for flight at high supersonic speeds. Rounded wing and tail leading edges were incorporated in this configuration as being desirable for high-speed operation from the standpoint of keeping the leading-edge temperatures within feasible limits. Test results showed that this configuration had maximum lift-drag ratios of 2.64 and 2.36 at Mach numbers of 4.06 and 6.86, respectively.

It appears that the drag of this configuration could be reduced, with consequent improvement of the maximum lift-drag ratios, by using a minimum-drag nose of higher fineness ratio and by using wing and tail surfaces with more highly swept leading edges. A triangular-wing model which incorporated these changes, and a trapezoidal-wing model, similar in plan form to that used in the tests reported in references 1 and 2, were tested in the Ames 10- by 14-inch wind tunnel to determine their comparative aerodynamic characteristics at Mach numbers from 3.00 to 6.28 and angles of attack up to  $15^\circ$ . Tests were also conducted on the trapezoidal-wing model with the minimum-drag nose (fineness ratio 5) to determine the drag reduction attributed to the nose modification. Since the nose of the body should be rounded to alleviate the local aerodynamic heating problem, the triangular-wing model was also tested with the minimum-drag nose blunted to a radius consistent with the blunting of the wing and tail leading edges.

## NOTATION

$C_D$	drag coefficient, $\frac{D}{qS}$
$C_L$	lift coefficient, $\frac{L}{qS}$
$C_m$	pitching-moment coefficient about wing centroid of area, $\frac{m}{qS\bar{c}}$
$\bar{c}$	mean aerodynamic chord of wing including portion submerged in fuselage
$D$	drag
$f$	fineness ratio, ratio of body length to maximum diameter
$L$	lift
$M$	free-stream Mach number

m	pitching moment
q	free-stream dynamic pressure
S	wing plan-form area, including area submerged in fuselage
$\bar{x}$	center-of-pressure location, percent body length from nose
$\alpha$	angle of attack

#### APPARATUS AND TESTS

The models were tested in the Ames 10- by 14-inch wind tunnel which is described in detail in reference 3. Aerodynamic forces and moments acting on the models were measured by a three-component strain-gage balance. Angles of attack up to  $5^\circ$  were obtained by rotating the model-balance assembly. Angles of attack greater than  $5^\circ$  were obtained by the use of bent-sting model supports. Axial forces acting on the model base, as determined by the difference between measured base pressures and free-stream static pressures, were subtracted from measured total forces. Thus, the data presented do not include the effects of base pressure.

Models used in the investigation were constructed of steel, with the tail surfaces permanently pinned to the cylindrical afterbody while the wings and nose sections were removable. Figure 1 shows the trapezoidal-wing model which is similar to that used in the tests reported in references 1 and 2, but with the following changes: (a) the four wedge-shaped tail surfaces have been replaced by three tail surfaces with the airfoil section shown in figure 1; and (b) the configuration has been changed from a mid-wing type to the low-wing type shown. The modification of this model in which the fineness-ratio-3 ogival nose is replaced by a fineness-ratio-5 minimum-drag nose is shown by the dashed lines on this figure. The ordinates for the minimum-drag nose (minimum drag for given length and volume, as determined from ref. 4) are given in table I. Figure 2 shows the triangular-wing model which has the same wing and tail surface areas as the trapezoidal-wing model, but has more highly swept leading edges as well as the fineness-ratio-5 minimum-drag nose. The modification to this model, as shown in this figure, consisted of shortening the fineness-ratio-5 minimum-drag nose to include a nose radius of  $1/10$  the maximum body radius. It has been indicated (ref. 5) that a sizable reduction in local heat-transfer rate can be achieved by sweeping the round leading edge of a wing or tail. In an attempt to obtain similar conditions of local heat input, therefore, the leading-edge radii of the triangular wing and tail have been reduced from those of the trapezoidal wing and tail as shown in figures 1 and 2.

Lift, drag, and pitching-moment coefficients as well as lift-drag ratios and center-of-pressure positions were determined for all models

at angles of attack to about  $15^\circ$  at Mach numbers of 3.00, 4.26, 5.04, and 6.28. The free-stream Reynolds numbers based on the lengths of the models were:

Mach number	Reynolds number, million	
	Basic trapezoidal- wing model	All other models
3.00	7.5	9.1
4.26	6.9	8.3
5.04	3.3	4.0
6.28	1.4	1.7

In the region of the test section where the models were located, the variation in Mach number did not exceed  $\pm 0.02$  at Mach numbers from 3.00 to 5.04 and  $\pm 0.04$  at Mach number 6.28. Deviations in free-stream Reynolds numbers did not exceed  $\pm 100,000$  from the values given. Estimated errors in the angle of attack due to uncertainties in corrections for stream angle and for deflection of the model-support system were  $\pm 0.2^\circ$ .

Precision of the experimental results was affected by uncertainties in the force measurements by the balance system and the determination of free-stream dynamic pressures and base pressures. These uncertainties result in maximum possible errors in the aerodynamic force and moment coefficients as shown in the following table:

<u>Mach number</u>	<u><math>C_D</math></u>	<u><math>C_L</math></u>	<u><math>C_m</math></u>
3.00	$\pm 0.003$	$\pm 0.002$	$\pm 0.005$
4.26	$\pm 0.003$	$\pm 0.002$	$\pm 0.005$
5.04	$\pm 0.004$	$\pm 0.003$	$\pm 0.008$
6.28	$\pm 0.006$	$\pm 0.005$	$\pm 0.015$

Accuracy of lift-drag ratios and centers of pressure will depend not only upon the accuracy of the force and moment coefficients but will, in general, be inversely proportional to the magnitude of these quantities. As such, the errors in the lift-drag ratios and centers of pressure will be comparatively large near zero angle of attack and will decrease as the angle of attack is increased.

## RESULTS AND DISCUSSION

Results of the tests on the four airplane-like configurations are presented in table II, where lift, drag, and pitching-moment coefficients, centers of pressure, and lift-drag ratios at various angles of attack are tabulated for the several test Mach numbers. In order to show the more important trends and comparisons of these aerodynamic parameters, certain data are also presented in graphical form. The variations of lift with angle of attack of the four models were found to be essentially the same at each test Mach number as may be seen in the tabulated test results. This similarity in lift characteristics is shown for the two basic models in figure 3. It can be shown from this figure that the initial lift-curve slope ( $dC_L/d\alpha$  for  $\alpha = 0$ ) is almost inversely proportional to  $\sqrt{M^2 - 1}$ , varying from a value of about 0.035 per degree at Mach number 3.00 to about 0.017 per degree at Mach number 6.28.

The variations of lift coefficient with drag coefficient, pitching-moment coefficient about the wing centroid of area, and the center of pressure in percent body length measured from the nose are shown in figure 4 for the two basic configurations and for the modified trapezoidal-wing model. The test results for the modified triangular-wing model are not included in this figure since they were approximately the same as those of the basic triangular-wing model, except for relatively small differences in drag coefficient as will be discussed later. In a comparison of the lift and drag coefficients, it can be seen that, for a given lift coefficient, the triangular-wing model has a consistently lower drag coefficient, and thus a higher lift-drag ratio, than does the basic trapezoidal-wing model. The corresponding curves for the modified trapezoidal-wing model show that, in the region of zero lift, about 40 to 50 percent of this difference is due to the use of the more slender minimum-drag nose. This drag reduction due to changing the nose shape is of the magnitude which would be predicted by Newtonian impact theory (ref. 6). The remainder of the drag reduction is due to the increased sweep angles and decreased radii of the wing and tail leading edges of the triangular-wing model.

The static longitudinal stability of each model tends to decrease with increasing Mach number as indicated by the less negative values of  $dC_m/dC_L$ . (See fig. 4.) The decreased stability is very likely due in part to a decrease in the effectiveness of the tail surfaces at higher Mach number. The possible need for additional stability at high Mach numbers was anticipated by the use of wedge-shaped tail surfaces on the model used in the tests reported in references 1 and 2. An alternate method for increasing stability at high Mach numbers, with possibly less drag penalty and fewer structural problems, would be to flare the rear portion of the cylindrical afterbody, as suggested in reference 7.

The variations of maximum lift-drag ratio with Mach number for the four configurations are presented in figure 5. It can be seen from this figure that the basic triangular-wing model has a maximum value of lift-drag ratio about 18 to 24 percent greater than that for the basic trapezoidal-wing model throughout the range of test Mach numbers. The addition of the fineness-ratio-5 minimum-drag nose to the trapezoidal-wing model increases the maximum lift-drag ratio about 7 to 11 percent in the range of the test Mach numbers. Although the drag of the modified triangular-wing model near zero lift is approximately the same as that of the basic triangular-wing model, as may be seen in the tabulated results, the drag of the modified model, except at a Mach number of 3.00, is slightly higher at the lift coefficients for which the lift-drag ratio is a maximum. This characteristic results in a decrease in maximum lift-drag ratio of about 5 percent at the highest test Mach number. Thus, at the higher Mach numbers, the heat-transfer characteristics are improved at the expense of a reduction of maximum lift-drag ratio.

The decrease in the maximum lift-drag ratios of all models as the Mach number is increased is due primarily to the increased skin-friction drag associated with the decrease of test Reynolds number. For these tests, the effects of skin-friction should be about the same for all models at corresponding Mach numbers and, therefore, should not influence the comparative results.

To facilitate model construction by allowing nose sections to be interchangeable, the afterbody length of all models was kept the same. As a result the models which employed minimum-drag nose sections are 2 inches longer than the basic trapezoidal-wing model and have correspondingly larger body volume. If the volumes of the longer models were made the same as that of the short model by reducing the afterbody length, there should be a negligible change in the lift and drag characteristics and an improvement in the stability characteristics due to a rearward shift in the center of pressure.

#### CONCLUSIONS

The aerodynamic characteristics of four airplane-like configurations, which have the same wing plan-form area, tail plan-form area, aspect ratio, and body diameter, have been determined at Mach numbers from 3.00 to 6.28 and at angles of attack up to  $15^\circ$ . From the results of these tests the following conclusions are drawn:

1. The lift characteristics of the models are about the same at each Mach number and, as would be expected, the lift-curve slopes decrease as the Mach number is increased.

2. The basic triangular-wing model had a greater nose fineness ratio and greater leading-edge sweep angles than the basic trapezoidal-wing model; both of these changes contributed substantial drag reductions.

3. The maximum lift-drag ratios of the basic triangular-wing model are about 18 to 24 percent higher than those of the basic trapezoidal-wing model.

4. A small increase in the bluntness of the minimum-drag nose was found to have a relatively small effect on the aerodynamic characteristics of the triangular-wing model at Mach number 3.00, but resulted in a progressive decrease in maximum lift-drag ratio with Mach number, so that a resultant decrease of about 5 percent occurred at Mach number 6.28.

5. The static longitudinal stability of the models tends to decrease as the Mach number is increased, probably due in part to a decreased effectiveness of the tail surfaces.

Ames Aeronautical Laboratory  
National Advisory Committee for Aeronautics  
Moffett Field, Calif., Mar. 24, 1955

#### REFERENCES

1. Dunning, Robert W., and Ulmann, Edward F.: Static Longitudinal and Lateral Stability Data from an Exploratory Investigation at Mach Number 4.06 of an Airplane Configuration Having a Wing of Trapezoidal Plan Form. NACA RM L55A21, 1955.
2. Penland, Jim A., Ridyard, Herbert W., and Fetterman, David E., Jr.: Lift, Drag, and Static Longitudinal Stability Data From an Exploratory Investigation at a Mach Number of 6.86 of an Airplane Configuration Having a Wing of Trapezoidal Plan Form. NACA RM L54L03b, 1955.
3. Eggers, A. J., Jr., and Nothwang, George J.: The Ames 10- by 14-Inch Supersonic Wind Tunnel. NACA TN 3095, 1954.
4. Eggers, A. J., Jr., Dennis, David H., and Resnikoff, Meyer M.: Bodies of Revolution for Minimum Drag at High Supersonic Airspeeds. NACA RM A51K27, 1952.
5. Eggers, Alfred J., Jr., Allen, H. Julian, and Neice, Stanford E.: A Comparative Analysis of the Performance of Long Range Hypervelocity Vehicles. NACA RM A54L10, 1955.
6. Grimmering, G., Williams, E. P., and Young, G. B. W.: Lift on Inclined Bodies of Revolution in Hypersonic Flow. Jour. Aero. Sci., vol. 17, no. 11, Nov. 1950, pp. 675 - 690.

~~CONFIDENTIAL~~

NACA RM A55C24

7. Eggers, A. J., Jr., and Syvertson, Clarence A.: Experimental Investigation of a Body Flare for Obtaining Pitch Stability and a Body Flap for Obtaining Pitch Control in Hypersonic Flight. NACA RM A54J13, 1955.

~~CONFIDENTIAL~~

TABLE I.- COORDINATES OF THE "MINIMUM-DRAG" NOSE SECTION  
[All values in inches.]

Abcissa	Ordinate
0	0.002
.100	.035
.200	.056
.300	.075
.400	.093
.600	.126
.800	.156
1.200	.211
1.600	.260
2.000	.303
2.400	.343
2.800	.379
3.200	.411
3.600	.440
4.000	.464
4.400	.483
4.800	.491
5.000	.500

TABLE II.- EXPERIMENTAL RESULTS

M	$\alpha$	$C_L$	$C_D$	$\frac{L}{D}$	$C_m$	$\bar{x}$	M	$\alpha$	$C_L$	$C_D$	$\frac{L}{D}$	$C_m$	$\bar{x}$
(a) Trapezoidal-wing model													
3.00	-1.0	-0.048	0.040	1.18	0.009	56.0	5.05	-2.0	-0.049	0.039	1.40	0	51.7
	0	-0.012	0.039	0.31	0.002	25.1		0	-0.010	0.033	0.32	-0.008	47.3
	1.0	0.084	0.040	0.61	-0.006	57.1		2.0	0.030	0.034	0.90	-0.006	56.1
	2.0	0.061	0.041	1.49	-0.015	57.2		2.9	0.055	0.036	1.56	-0.009	55.2
	4.1	0.134	0.049	2.76	-0.031	56.9		5.0	0.099	0.042	2.34	-0.015	55.0
	6.7	0.213	0.064	3.33	-0.050	56.9		7.0	0.148	0.053	2.76	-0.021	54.8
	8.7	0.266	0.083	3.46	-0.064	56.7		8.0	0.176	0.062	2.82	-0.026	56.1
	10.7	0.369	0.109	3.35	-0.085	56.8		10.0	0.230	0.079	2.93	-0.046	56.1
	12.7	0.444	0.146	3.20	-0.113	57.1		12.1	0.280	0.100	2.86	-0.061	56.3
	13.8	0.495	0.162	3.06	-0.121	57.0							
	14.8	0.535	0.184	2.91	-0.132	57.0							
4.26	-2.0	-0.096	0.035	1.61	0.004	53.2	6.26	-2.0	-0.040	0.037	1.08	0.001	52.4
	0	-0.012	0.034	0.37	0.001	54.4		0	-0.009	0.039	0.24	0.001	54.8
	1.9	0.037	0.034	1.07	-0.006	55.6		2.0	0.026	0.036	0.73	-0.006	46.3
	3.1	0.068	0.037	1.81	-0.014	56.3		2.9	0.045	0.036	1.25	-0.003	53.2
	5.1	0.117	0.045	2.61	-0.021	55.7		4.9	0.082	0.042	1.95	-0.006	55.2
	7.0	0.178	0.062	3.06	-0.033	55.9		6.9	0.129	0.052	2.43	-0.017	54.7
	8.2	0.206	0.069	3.18	-0.042	56.2		7.9	0.143	0.057	2.53	-0.028	52.9
	10.2	0.264	0.084	3.15	-0.052	56.0		9.9	0.189	0.071	2.66	-0.013	53.3
	12.1	0.323	0.107	3.02	-0.062	55.9		11.8	0.246	0.089	2.77	-0.033	54.6
								12.9	0.270	0.100	2.70	-0.031	54.2
(b) Modified trapezoidal-wing model													
3.00	-1.0	-0.047	0.036	1.29	0.006	62.6	5.05	-2.0	-0.048	0.028	1.70	0.003	58.8
	0	-0.011	0.035	0.32	0	60.3		0	-0.008	0.027	0.31	-0.003	52.5
	1.0	0.068	0.039	0.80	-0.007	64.7		2.0	0.034	0.027	1.22	-0.002	61.4
	2.0	0.063	0.036	1.73	-0.014	64.2		2.9	0.058	0.033	1.76	-0.003	61.2
	4.1	0.136	0.043	3.15	-0.026	63.7		5.0	0.103	0.040	2.58	-0.006	61.1
	6.7	0.221	0.062	3.57	-0.043	63.7		7.0	0.154	0.051	3.02	-0.011	61.4
	8.2	0.298	0.082	3.63	-0.056	63.5		9.0	0.179	0.059	3.04	-0.017	61.9
	10.7	0.382	0.100	3.84	-0.072	63.2		10.0	0.235	0.076	3.10	-0.022	61.6
	12.8	0.475	0.144	3.28	-0.089	63.2		12.1	0.296	0.093	3.03	-0.029	61.8
	14.9	0.561	0.188	2.98	-0.103	63.4							
4.26	-2.0	-0.096	0.031	1.82	0.003	61.0	6.26	-2.0	-0.042	0.033	1.27	-0.006	57.4
	0	-0.011	0.028	0.41	0.002	63.2		0	-0.011	0.031	0.35	-0.001	58.9
	1.9	0.038	0.029	1.30	-0.003	61.7		2.0	0.025	0.032	0.79	0.003	57.8
	3.1	0.069	0.033	2.09	-0.010	62.7		2.9	0.047	0.035	1.34	0.015	54.2
	5.0	0.118	0.040	2.95	-0.013	62.8		4.9	0.088	0.043	2.05	-0.004	60.4
	7.0	0.177	0.051	3.46	-0.026	62.8		6.9	0.131	0.053	2.45	-0.009	60.8
	8.2	0.217	0.063	3.44	-0.028	62.3		7.9	0.145	0.053	2.76	-0.003	59.8
	10.4	0.277	0.086	3.22	-0.034	62.3		9.9	0.193	0.064	3.03	0.003	59.8
	12.5	0.335	0.111	3.02	-0.030	61.7		11.9	0.246	0.081	3.04	-0.005	60.5
								12.9	0.273	0.092	2.96	-0.011	60.8
(c) Triangular-wing model													
3.00	-1.0	-0.043	0.029	1.48	0.007	63.6	5.05	-2.0	-0.042	0.026	1.93	0.002	61.1
	0	-0.008	0.028	0.28	0.002	64.6		0	-0.010	0.024	0.44	0.003	67.3
	1.0	0.029	0.028	1.03	-0.006	64.0		1.0	0.010	0.024	0.43	0.003	63.5
	2.0	0.066	0.030	2.24	-0.014	64.4		2.0	0.031	0.025	1.25	-0.002	55.1
	4.1	0.140	0.038	3.71	-0.030	64.6		2.9	0.058	0.025	2.36	-0.007	62.7
	6.7	0.220	0.056	3.96	-0.043	64.1		5.0	0.104	0.033	3.19	-0.009	61.9
	8.7	0.295	0.074	3.95	-0.059	64.3		7.0	0.154	0.044	3.93	-0.016	62.3
	10.7	0.369	0.101	3.65	-0.070	64.0		8.0	0.183	0.050	3.67	-0.022	62.4
	12.7	0.433	0.133	3.41	-0.088	64.0		10.0	0.239	0.067	3.56	-0.029	62.2
	13.8	0.482	0.152	3.21	-0.095	63.6		12.1	0.300	0.089	3.38	-0.032	62.3
	14.8	0.526	0.173	3.04	-0.099	63.5							
4.26	-2.0	-0.095	0.026	2.14	0.003	61.2	6.26	-2.0	-0.041	0.030	1.39	0.003	61.8
	0	-0.008	0.023	0.35	0.001	58.6		0	-0.007	0.027	0.27	0.006	76.9
	1.0	0.015	0.024	0.64	-0.001	61.6		1.0	0.009	0.027	0.35	0.006	46.9
	1.9	0.040	0.025	1.61	-0.004	61.9		2.0	0.027	0.028	0.97	0.009	56.3
	3.1	0.072	0.026	2.68	-0.012	61.5		2.9	0.046	0.027	1.69	0.004	58.3
	5.0	0.118	0.032	3.70	-0.012	62.2		4.9	0.086	0.033	2.98	0.004	60.9
	7.0	0.178	0.045	3.97	-0.026	63.2		6.9	0.128	0.040	3.18	0.002	59.9
	8.2	0.210	0.056	3.78	-0.022	62.2		7.9	0.131	0.044	3.26	-0.016	62.5
	10.2	0.272	0.076	3.60	-0.027	62.1		9.9	0.171	0.046	3.30	-0.009	61.3
	12.1	0.331	0.099	3.35	-0.028	61.8		11.9	0.201	0.061	3.28	-0.015	61.6
								12.9	0.251	0.080	3.15	-0.021	61.8
(d) Modified triangular-wing model													
3.00	-1.0	-0.048	0.029	1.45	0.007	63.6	5.05	-2.0	-0.047	0.024	1.99	0	59.9
	0	-0.007	0.028	0.25	0.001	62.8		0	-0.009	0.022	0.38	-0.003	51.8
	1.0	0.030	0.028	1.06	-0.006	64.4		1.0	0.011	0.022	0.51	-0.004	67.6
	2.0	0.067	0.030	2.19	-0.014	64.6		2.0	0.032	0.023	1.38	-0.004	62.9
	4.1	0.141	0.039	3.65	-0.031	64.6		2.9	0.056	0.026	2.25	-0.004	61.4
	6.7	0.220	0.055	3.96	-0.044	64.2		5.0	0.103	0.033	3.10	-0.008	61.6
	8.7	0.296	0.075	3.95	-0.059	64.1		7.0	0.153	0.045	3.42	-0.013	61.8
	10.7	0.375	0.100	3.72	-0.071	64.0		8.0	0.182	0.052	3.70	-0.022	62.6
	12.8	0.457	0.132	3.46	-0.081	64.1		10.0	0.237	0.070	3.40	-0.028	62.5
	14.9	0.532	0.171	3.10	-0.092	63.6		12.1	0.296	0.093	3.20	-0.039	62.8
4.26	-2.0	-0.095	0.025	2.23	0.005	61.8	6.26	-2.0	-0.042	0.027	1.56	-0.002	59.3
	0	-0.009	0.022	0.42	0.001	61.4		0	-0.009	0.024	0.38	0.002	64.2
	1.9	0.015	0.022	0.67	-0.002	62.3		1.0	0.008	0.024	0.31	0.004	48.5
	1.9	0.040	0.024	1.65	-0.005	62.8		2.0	0.025	0.025	0.98	0.002	58.7
	3.1	0.070	0.027	2.79	-0.010	63.0		2.9	0.043	0.026	1.70	0.004	58.1
	5.0	0.121	0.035	3.43	-0.015	62.7		4.9	0.083	0.032	2.57	-0.005	61.3
	7.0	0.179	0.047	3.78	-0.026	63.0		6.9	0.126	0.042	2.94	-0.001	59.9
	8.2	0.217	0.058	3.75	-0.026	63.5		7.9	0.126	0.042	2.97	-0.018	63.1
	10.2	0.276	0.078	3.54	-0.040	63.0		9.9	0.153	0.048	3.06	-0.009	61.4
	12.1	0.337	0.103	3.27	-0.043	62.7		11.9	0.203	0.064	3.11	-0.017	62.0
								12.9	0.258	0.084	2.95	-0.024	62.1

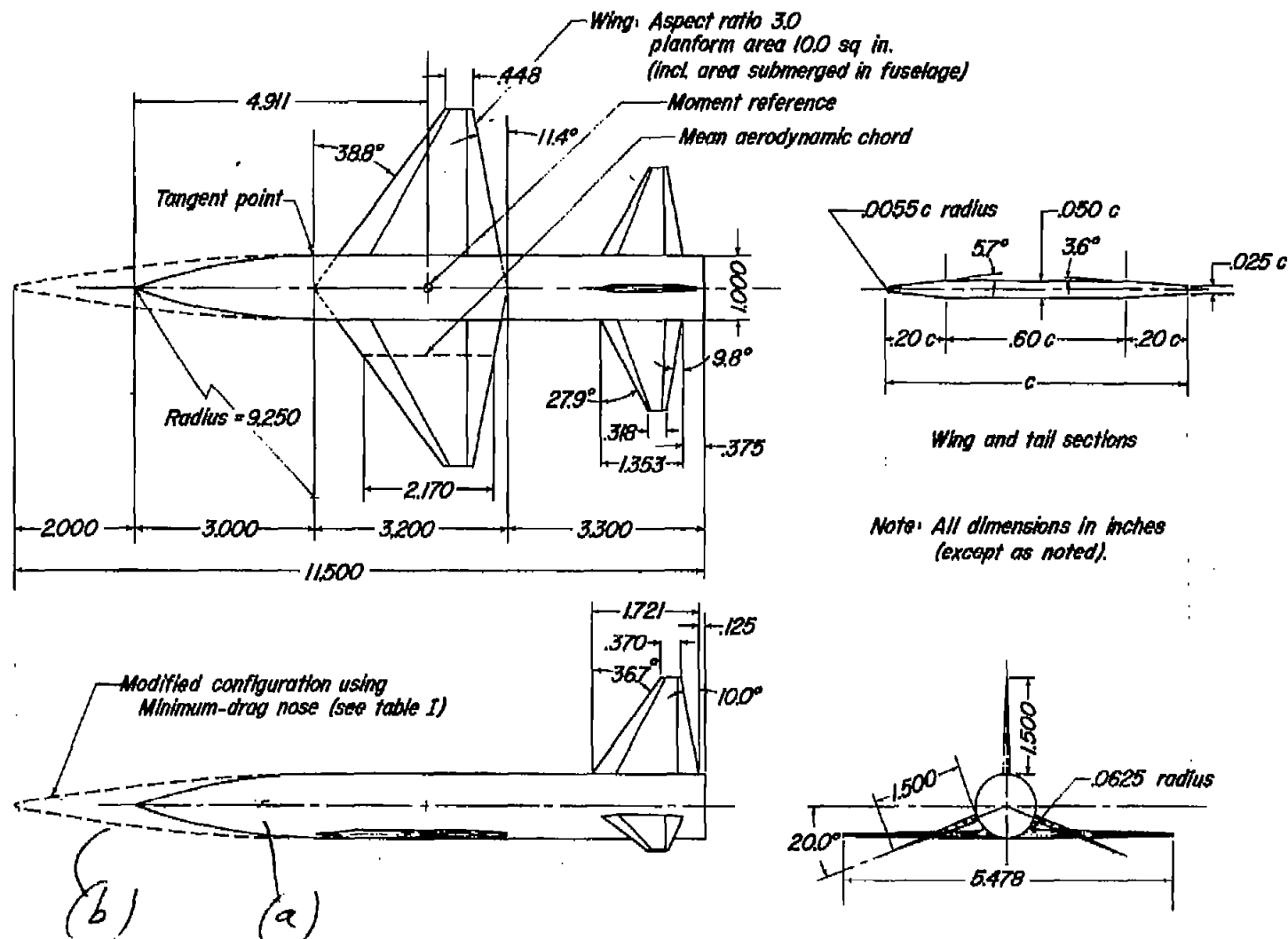


Figure 1.- Dimensions of trapezoidal-wing model.

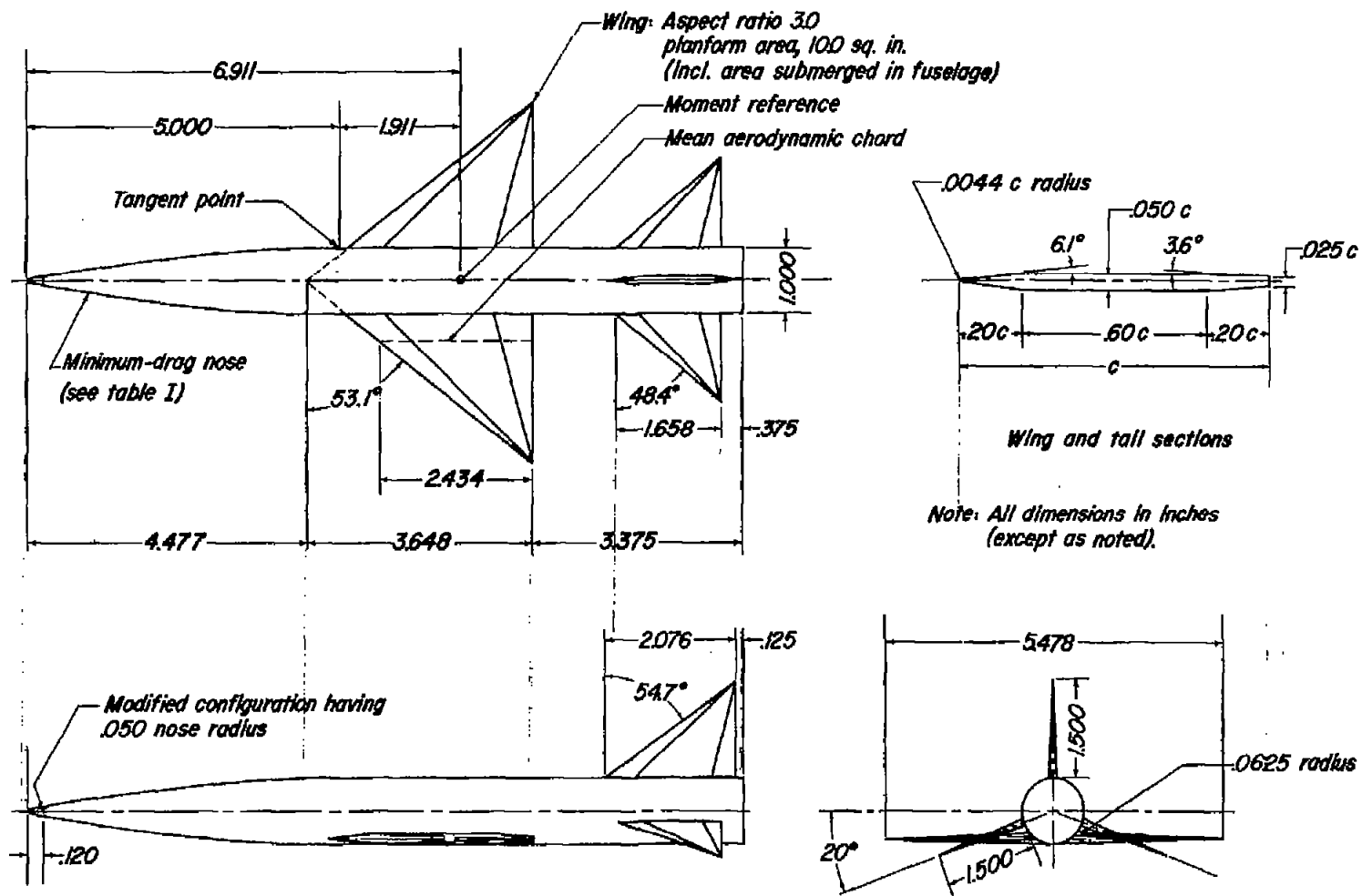


Figure 2.— Dimensions of triangular-wing model.

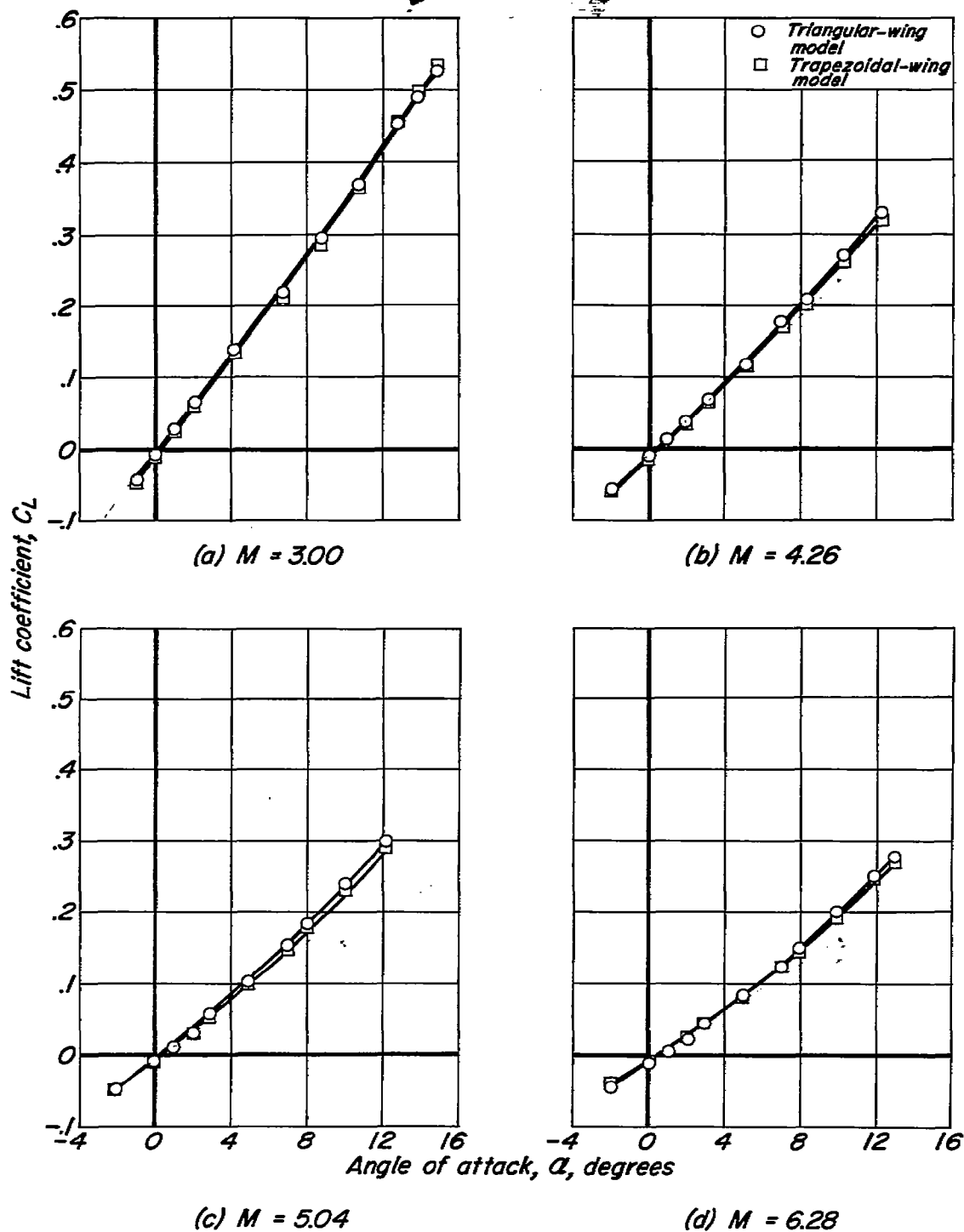


Figure 3.— Variation of lift coefficient with angle of attack for basic test models.

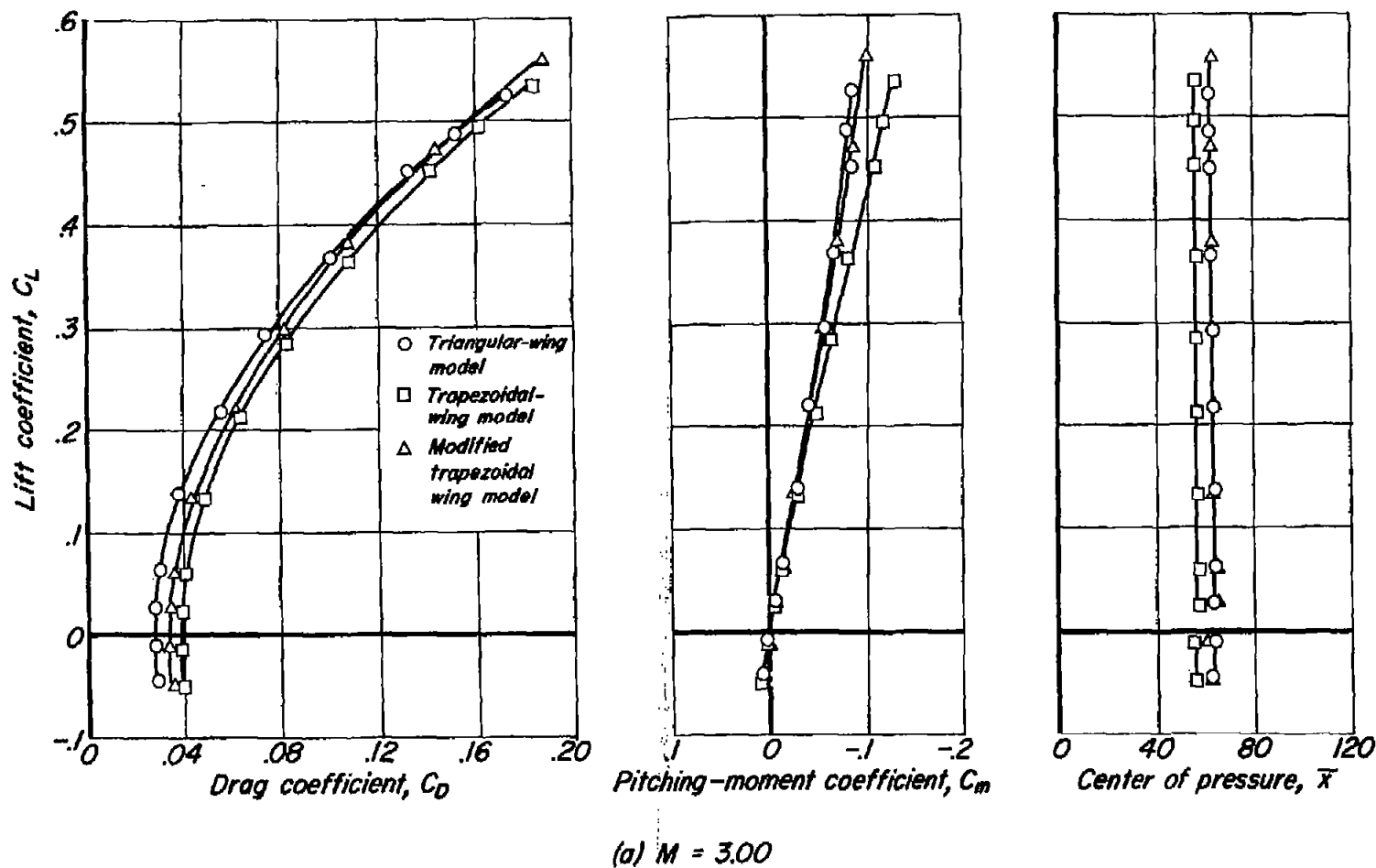
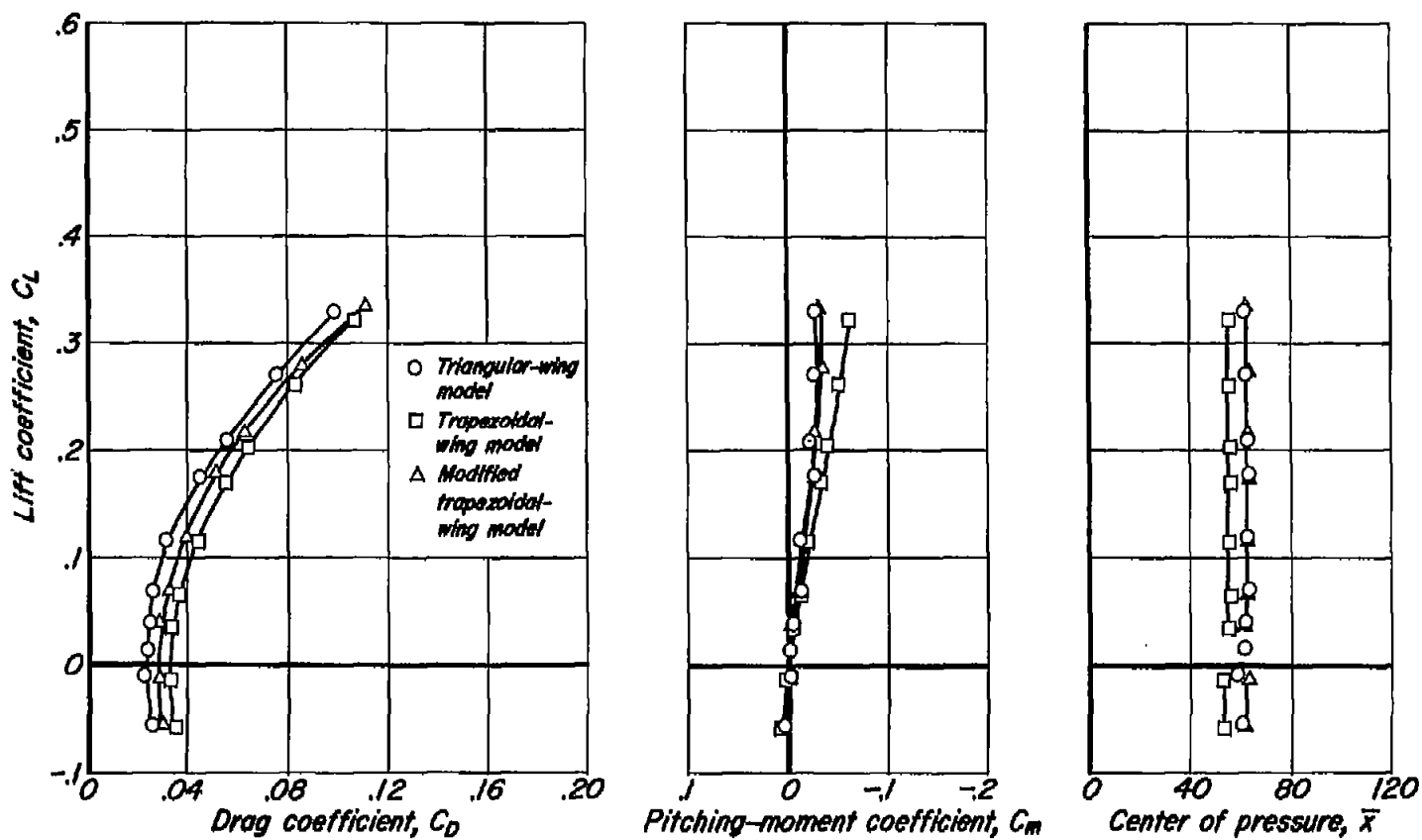


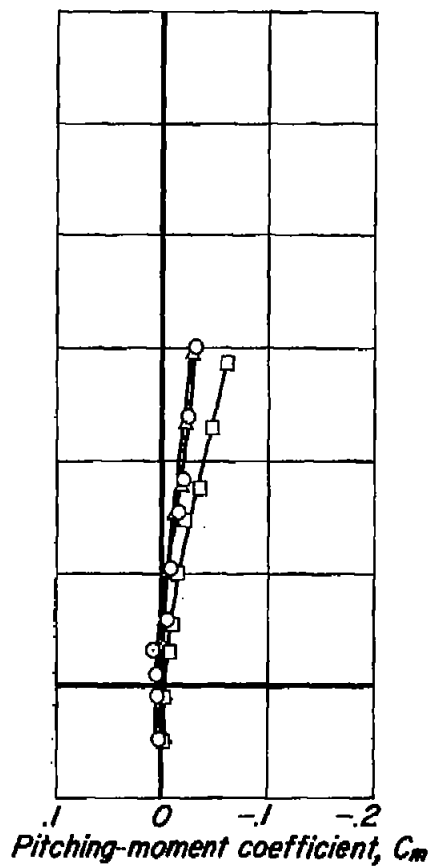
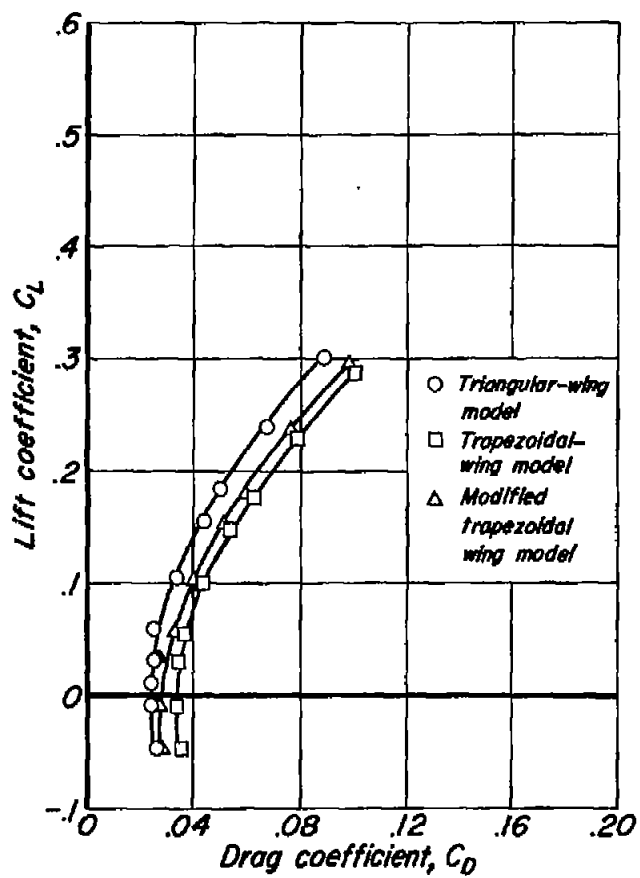
Figure 4.— Aerodynamic characteristics of three test models (modified triangular-wing model omitted).



(b)  $M = 4.26$

Figure 4.- Continued.

CONFIDENTIAL



(c)  $M = 5.04$

Figure 4.- Continued.

CONFIDENTIAL

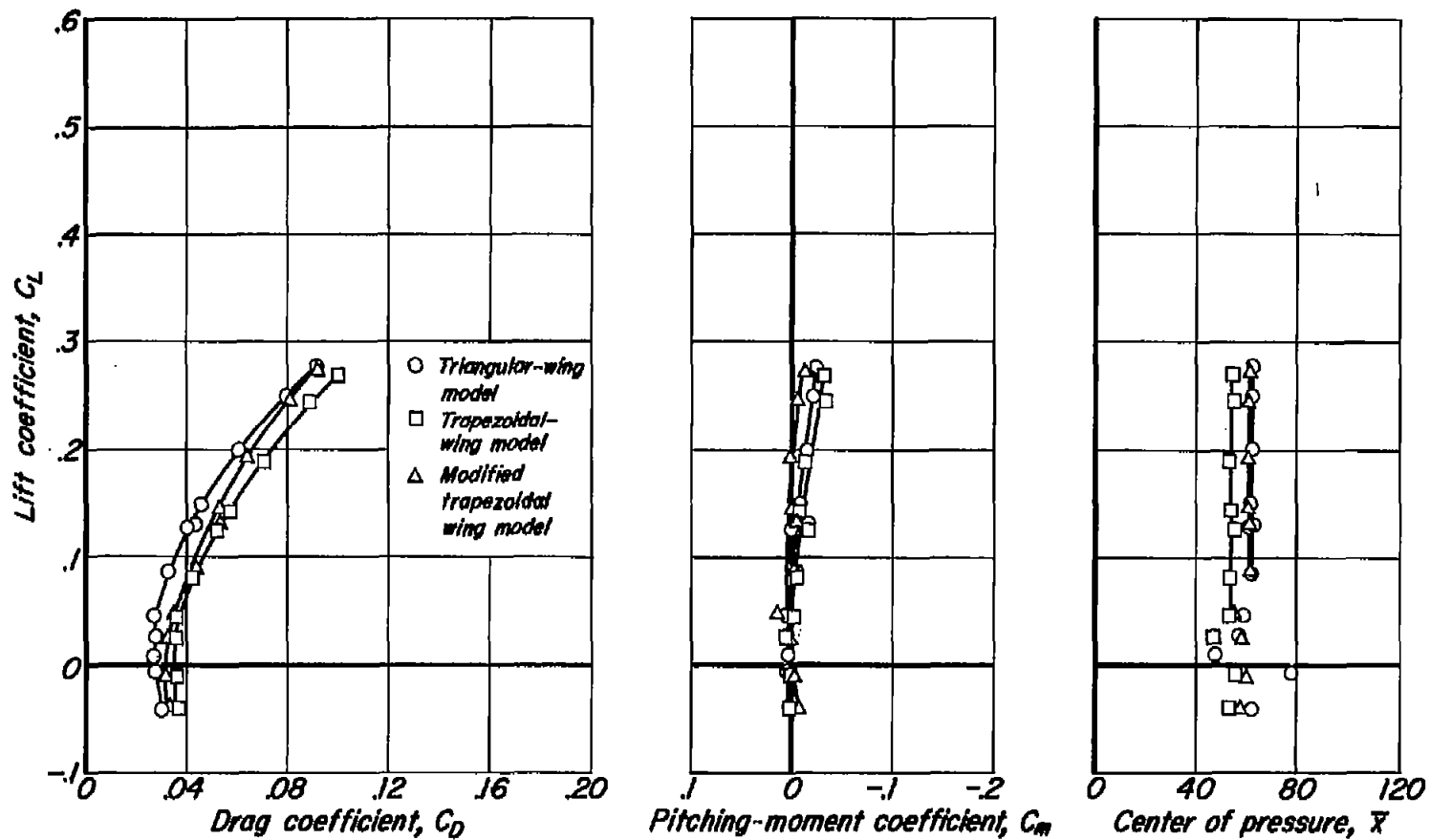
(d)  $M = 6.28$ 

Figure 4.- Concluded.

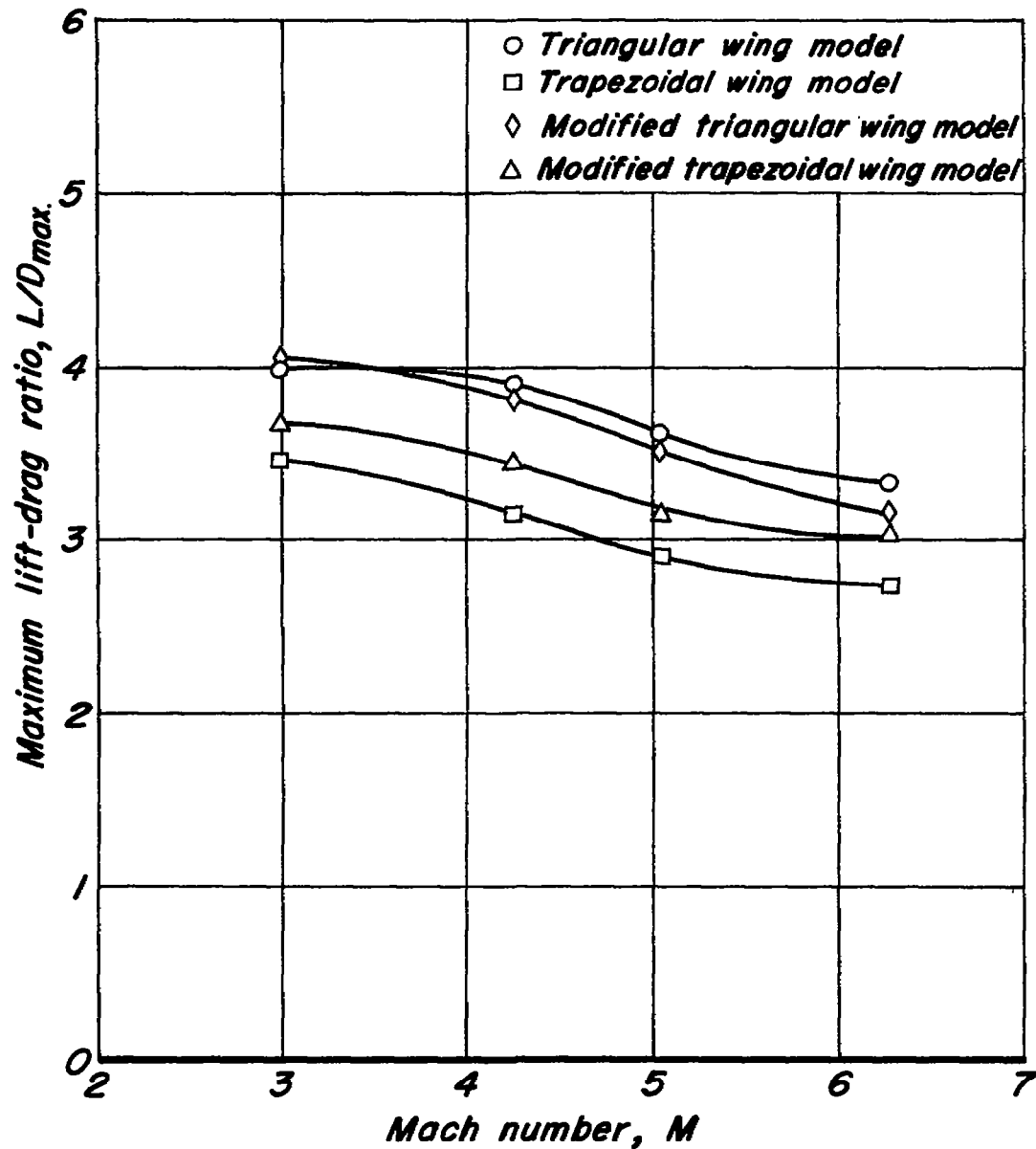


Figure 5.- Variation of maximum lift-drag ratio with Mach number for all models.